On-demand generation of entanglement of atomic qubits via optical interferometry

Y. P. Huang and M. G. Moore
Department of Physics and Astronomy, Michigan State University, East Lansing, Michigan 48824, USA
(Received 8 September 2006; published 31 March 2008)

The problem of on-demand generation of entanglement between single-atom qubits via a common photonic channel is examined within the framework of optical interferometry. As expected, for a Mach-Zehnder interferometer with coherent laser beam as input, a high-finesse optical cavity is required to overcome sensitivity to spontaneous emission. We show, however, that with a twin-Fock input, useful entanglement can in principle be created without cavity enhancement. Both approaches require single-photon resolving detectors, and best results would be obtained by combining both cavity feedback and twin-Fock inputs. Such an approach may allow a fidelity of 0.99 using a two-photon input and currently available mirror and detector technology. In addition, we study interferometers based on NOON states, i.e., maximally entangled N-particle states, and show that they perform similarly to the twin-Fock states, yet without the need for high-precision photodetectors. The present interferometrical approach can serve as a universal, scalable circuit element for quantum information processing, from which fast quantum gates, deterministic teleportation, entanglement swapping, etc., can be realized with the aid of single-qubit operations.

DOI: 10.1103/PhysRevA.77.032349 PACS number(s): 03.67.Hk, 03.67.Mn, 42.50.Dv

I. INTRODUCTION

Practical quantum information processing will rely on deterministic computational gates and high-fidelity communication protocols that operate successfully on-demand [1–3]. This requires real-time generation of entanglement among arbitrary qubits performed at near-unit success probability and fidelity. For atom-type qubits, this entanglement can be generated either via a photonic channel, utilizing entangled photon pairs [3,4] or cavity-decay photons [5–8], or an atomic channel as in recent trapped-ion experiments [9,10]. For high-speed quantum computation and/or long-distance communication, a photonic quantum channel is clearly ideal, as photons are robust carriers of quantum information that travel at the speed of light. Since isolated trapped-atomic qubits have long coherence times and are easily manipulated with electromagnetic fields, it is of general interest to consider the problem of creating entanglement between two isolated atomic qubits via their mutual interaction with a single photonic channel. The primary obstacle to such a protocol lies in the problem of eliminating spontaneous emission while obtaining a sufficiently strong atom-photon interaction. Recent attempts to overcome this difficulty have primarily relied on the use of collective-state qubits in atomic ensembles to enhance the dipole moment of the qubit [11–13]. This enhancement effect has allowed Duan, Cirac, Zoller, and Polzik to implement a quantum teleportation scheme between two atomic samples, where a coherent beam is passed successively through and the entanglement is generated by measuring its final Faraday-rotation angle [11]. Very recently, a probabilistic scheme to entangle two distant quantum dots using cavity enhancement has been proposed using bright coherent light via homodyne detection and postselection [14].

In this paper, we investigate an approach in which *single*-atom qubits are deterministically entangled by use of an optical interferometer, thus avoiding collisional decoherence mechanisms inherent in atomic ensembles. It is well known that the backaction of a single atom onto a focused laser pulse is very weak, so that generating useful atom-photon entanglement in this manner will generally fail due to spontaneous emission [15]. Our goal, however, is to overcome this difficulty by using the extreme sensitivity of sub-shot-noise interferometers [16–24] to detect the weak phase imprinted on the forward scattered light in the regime where spontaneous emission is negligible. In addition, we also consider the more generic approach of using high-finesse optical resonators [25,26] to enhance the atom-photon interaction. Our interferometry apparatus follows the Faraday-rotation scheme of Duan, Cirac, Zoller, and Polzik [11], with the collective atomic ensembles replaced by single trapped atoms, and with the coherent light replaced by a highly nonclassical many-photon state. We first show that for a Mach-Zehnder (MZ) interferometer with coherent input, a high-finesse Q-switch cavity is always necessary, and to achieve a fidelity of $f=0.99$ requires an optical cavity which cycles the photon for $M=10^5-10^6$ times. If the coherent state input is replaced with a twin-Fock (TF) input state, however, we find that a cavity is in principle no longer required. Cavity feedback may still provide additional improvement in performance. For example, $f=0.99$ can be achieved if we use the TF state with 4×10^4 photons and no cavity, or only two photons and cavities with $M=2\times10^4$. The latter requires a single photon-on-demand [27] injected into each interferometer input, with an accurate measurement of the two-photon output state, which appears within the realm of experimental feasibility. Both MZ-interferometer-based approaches require detectors with single-photon resolution [28]. This requirement, however, can be overcome by employing a non-MZ interferometer based on NOON states, i.e., maximally entangled N-particle states, and nonlinear beamsplitters. Such an interferometer yields a sensitivity close to the TF state in detecting phase imbalance, and thus can achieve similar performance without counting single photons. While the TF and NOON states have recently been shown as unable to measure any phase below shot noise in a single measurement [18,29,30], our present work shows that single measurements

with these states can still be highly useful as "quantum switches" with Heisenberg-limited sensitivity.

Our proposed interferometry approach to entangle atomic qubits can be performed on-demand and is scalable. We envision generalizing such a device to a complete set of quantum information processing protocols whereby stationary single-atom qubits are held in isolated traps, with arbitrary single-atom and multiatom operations achieved via sequences of light pulses guided among the atoms and into detectors by fast optical switching. The goal of this paper is to perform a theoretical analysis of interferometrical generation of entanglement between two arbitrary qubits, and to determine the fundamental limitations imposed by quantum mechanics.

The paper is organized as follows. In Sec. II, we present a basic model of the interferometrical generation of entanglement between two atomic qubits. In Sec. III, we study two MZ-interferometrical approaches using the coherent and the TF input light fields, respectively. Then in Sec. IV, we investigate an alternative approach employing NOON states and nonlinear beamsplitters. In Sec. V, as examples, we briefly show how the present scheme can be applied to realize deterministic teleportation, multisite entanglement, and entanglement swapping. This is followed by a short discussion and conclusion in Sec. VI.

II. MODEL

In our scheme, a single pulse of light is passed through an optical interferometer, with the different "arms" of the interferometer corresponding to different photon polarization states. The beam passes through two atomic qubits, i.e., trapped ions, neutral atoms, and/or quantum dots, such that each polarization state interacts with a different internal atomic state. This can be achieved using an "X"-type scheme, as described in [11], in which the Zeeman sublevels of an $F=1/2$ ground state form the qubit, or in a Λ-type level scheme, with the $m=\pm 1$ states of an $F=1$ ground state forming the qubits. In both cases, the arms of the interferometer would correspond to orthogonal circular polarization states. The interferometer output is determined by a state-dependent phase shift acquired via the atom-photon interaction. This requires a large detuning from the atomic resonance, as there is no phase acquired on resonance. Measurement of a phase imbalance at the interferometer output cannot determine which qubit contributed the phase shift, resulting in entanglement between them.

We consider atomic qubits based on two degenerate hyperfine states, arbitrarily labeled as $|0\rangle$ and $|1\rangle$. For a general consideration, our goal is to entangle two uncorrelated qubits, labeled x and y, which are initially in states of $|\psi_x\rangle$, $|\psi_y\rangle$, where

$$|\psi_\mu\rangle = \chi_0^\mu|0\rangle_\mu + \chi_1^\mu|1\rangle_\mu, \tag{1}$$

and $\mu\in\{x,y\}$. The qubits are placed inside an optical interferometer with the setup depicted in Fig. 1, where the states $|0\rangle_x$ and $|0\rangle_y$ interact with photons in the upper arm of the interferometer, while $|1\rangle_x$ and $|1\rangle_y$ interact with the lower. Such interaction is represented by the qubit-photon interaction propagator,

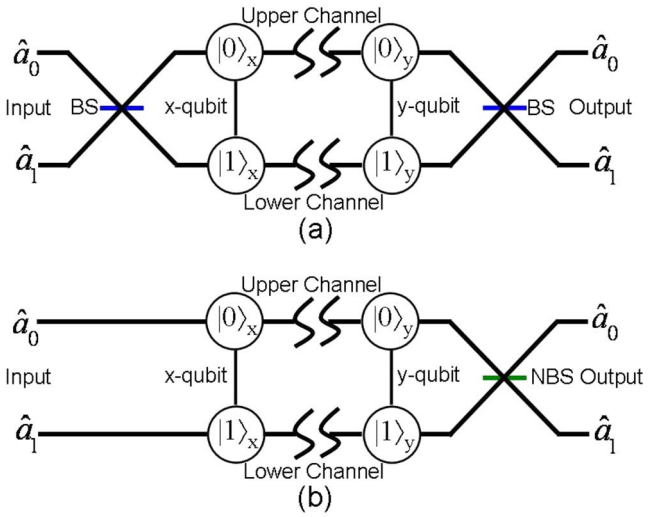

FIG. 1. (Color online) Schematic setup of entanglement generation with optical interferometers. (a) shows the setup with the MZ interferometer which consists of two linear 50/50 beamsplitters (BS). (b) shows the setup with the NOON-state interferometer consisting of only one nonlinear beamsplitter (NBS).

$$\hat{U}_\mu = \exp[-i\theta(\hat{a}_0^\dagger\hat{a}_0\hat{c}_{\mu 0}^\dagger\hat{c}_{\mu 0} + \hat{a}_1^\dagger\hat{a}_1\hat{c}_{\mu 1}^\dagger\hat{c}_{\mu 1})], \tag{2}$$

where $\hat{c}_{\mu m}$ is the annihilation operator for an atom at location $\mu\in\{x,y\}$ in internal state $m\in\{0,1\}$. This interaction operator is valid in the far-off-resonance regime, where the electronically excited state can be adiabatically eliminated. The interaction is governed by the phase shift

$$\theta = \frac{|d\mathcal{E}(\omega)|^2\tau}{\hbar^2\Delta}, \tag{3}$$

where τ is the atom-photon interaction time, Δ is the detuning between the laser and atomic resonance frequencies, d is the electric dipole moment, and $\mathcal{E}(\omega)=\sqrt{\hbar\omega/(2\varepsilon_0 V)}$ is the "electric field per photon" for laser frequency ω and mode-volume V. Introducing the spontaneous emission rate $\Gamma = d^2\omega^3/(3\pi\varepsilon_0\hbar c^3)$, taking the photon mode as having length L and width W (at the location of the atom), and taking the interaction time as $\tau=L/c$, we arrive at the single-atom phase shift

$$\theta = \frac{3}{8\pi}\left[\frac{\lambda}{W}\right]^2\frac{\Gamma}{\Delta}, \tag{4}$$

where λ is the laser wavelength. This is the phase shift acquired by an off-resonant photon forward-scattered by a single atom, and is independent of the pulse length.

The interferometer output is then determined by the phase shift acquired via the atom-photon interaction. Introducing the qubit-pair basis $|ij\rangle \equiv |i\rangle_x\otimes|j\rangle_y$ with $i,j=0,1$, the states $|01\rangle$ and $|10\rangle$ both correspond to a balanced interferometer with zero net phase shift, and thus constitute a "balanced" qubit-pair subspace. In contrast, the states $|00\rangle$ and $|11\rangle$ have equal and opposite nonzero phase shifts, and thus constitute an "imbalanced" subspace. Measuring the photon number distribution at the interferometer output distinguishes be-

tween zero and nonzero magnitudes of the phase shifts, and thus collapses the qubits onto the balanced or imbalanced subspaces, based on which entanglement between the two is established.

III. MZ INTERFEROMETER

The basic setup for entanglement generation using the MZ interferometer is shown in Fig. 1(a). The MZ interferometer consists of two 50/50 linear beamsplitters. The input light field is bifurcated at the first beamsplitter, guided to interact sequentially with the qubits, and then recombined at the second beamsplitter. Passage of photons through the MZ interferometer can be described by the propagator,

$$\hat{U} = \hat{U}_{BS}\hat{U}_y\hat{U}_x\hat{U}_{BS}, \tag{5}$$

where $\hat{U}_{BS}$ is the 50/50 beamsplitter propagator,

$$\hat{U}_{BS} = \exp[-i(\hat{a}_0^\dagger\hat{a}_1 + \hat{a}_1^\dagger\hat{a}_0)\pi/4]. \tag{6}$$

Without specifying the input light field, the initial states of the system can be written in a general form

$$|\Psi_i\rangle = \Phi(\hat{a}_0^\dagger,\hat{a}_1^\dagger)|0\rangle \otimes |\psi_x\rangle \otimes |\psi_y\rangle, \tag{7}$$

where $|0\rangle$ is the electromagnetic vacuum state and $\Phi(\hat{a}_0^\dagger,\hat{a}_1^\dagger)$ defines the light field. The state of the system at the interferometer output is then given by

$$|\Psi_f\rangle = \hat{U}|\Psi_i\rangle = \Phi(\hat{U}\hat{a}_0^\dagger\hat{U}^\dagger,\hat{U}\hat{a}_1^\dagger\hat{U}^\dagger)|0\rangle \otimes |\psi_x\rangle \otimes |\psi_y\rangle. \tag{8}$$

Introducing dual-qubit spin operator

$$\sigma_z = \frac{1}{2}\sum_{\mu=S,T}(\hat{c}_{\mu 0}^\dagger\hat{c}_{\mu 0} - \hat{c}_{\mu 1}^\dagger\hat{c}_{\mu 1}), \tag{9}$$

we find that

$$\hat{U}\hat{a}_0^\dagger\hat{U}^\dagger = ie^{i\theta}[\sin(\theta\sigma_z)\hat{a}_0^\dagger + \cos(\theta\sigma_z)\hat{a}_1^\dagger], \tag{10}$$

$$\hat{U}\hat{a}_1^\dagger\hat{U}^\dagger = ie^{i\theta}[\cos(\theta\sigma_z)\hat{a}_0^\dagger - \sin(\theta\sigma_z)\hat{a}_1^\dagger]. \tag{11}$$

The final state can now be rewritten as

$$|\Psi_f\rangle = \sum_{i,j=0,1}\chi_i^x\chi_j^y|\Phi(\theta_{ij})\rangle \otimes |ij\rangle, \tag{12}$$

where $|\Phi(\theta_{ij})\rangle$ is the output light field in the presence of qubits-dependent interferometer phase $\theta_{ij}=\theta\times(1-i-j)$. It is now evident that the interferometer output is determined by the joint states of the qubits. The states $|01\rangle$ and $|10\rangle$ result in zero phase shifts with $\theta_{01}=\theta_{10}=0$, while $|00\rangle$ and $|11\rangle$ result in equation and opposite phases with $\theta_{00}=-\theta_{11}=\theta$. If the interferometer is incapable of distinguishing positive and negative phases, a measurement of the output light field will therefore collapse the qubits onto either balanced or imbalanced subspaces, and in this way generate entanglement between them.

We note that our MZ interferometer scheme is closely related to the Faraday-rotation scheme of Duan *et al.* [11], which effectively replaces the first beamsplitter with a linear-polarized initial coherent state. In fact, for the special case of a circularly polarized coherent state at one input port and vacuum at the other, the present MZ interferometry scheme maps directly to the Faraday-rotation scheme. As we will show next, an interferometer of this class is limited to shot-noise sensitivity, and will thus not work when the ensembles are replaced by single atoms without the introduction of extremely high-finesse optical resonators. Viewing the Faraday-rotation scheme instead as a MZ interferometer clearly highlights the possibility to incorporate nonclassical input states to achieve sub-shot-noise sensitivity, which is the focus of the present manuscript.

A. Coherent-state input

For the coherent-state input, the upper channel, described by creation operator $\hat{a}_0^\dagger$, is initially in a coherent state, while the lower channel $\hat{a}_1^\dagger$ is in the vacuum state. A detector is used to count the photons coming from the upper output channel, while output in the lower channel is unmeasured. A null result, meaning zero photons detected, results in the qubits collapsing onto the balanced subspace,

$$\chi_0^x\chi_1^y|01\rangle + \chi_1^x\chi_0^y|10\rangle + |\varepsilon\rangle, \tag{13}$$

where $|\varepsilon\rangle$ is the intrinsic state error due to the possibility of a false null result. This error, which adds imbalanced states to the desired balanced subspace, sets the upper limit of the obtainable teleportation fidelity. If $n\neq 0$ photons are detected, the qubits will collapse onto imbalanced subspace,

$$\chi_0^x\chi_0^y|00\rangle + \chi_1^x\chi_1^y(-1)^n|11\rangle, \tag{14}$$

without intrinsic error. We note that the possibility of a dark count *will* introduce an analogous error, but this error rate is governed by technical aspects of the photodetector, and is presumably not an intrinsic quantum error.

To derive these results for coherent input state, the initial state of the complete system is given by Eq. (7), with

$$\Phi_i(\hat{a}_0^\dagger,\hat{a}_1^\dagger) = e^{-\alpha\hat{a}_0^\dagger + \alpha^*\hat{a}_0}. \tag{15}$$

Following Eq. (16), the state of the system at the interferometer output is obtained as

$$|\Psi_f\rangle = \sum_{i,j=0,1}\chi_i^x\chi_j^y|ij\rangle \otimes |\bar{\alpha}\sin\theta_{ij}\rangle_0 \otimes |\bar{\alpha}\cos\theta_{ij}\rangle_1, \tag{16}$$

where $\bar{\alpha}=-i\alpha e^{i\theta}$ and the states $|\alpha\rangle_{0,1}$ indicate optical coherent states for the upper and lower interferometer outputs, respectively. Expanding the upper channel onto photon number-eigenstates and making the small-angle approximation gives

$$|\Psi_f\rangle = \sum_{n=0}^{\infty}|n\rangle_0 \otimes |\bar{\alpha}\rangle_1 \otimes |\phi_n\rangle_{xy}, \tag{17}$$

where $|n\rangle_0$ indicates a state with n photons in the upper output, and

$$|\phi_0\rangle_{xy} = \chi_0^x\chi_1^y|01\rangle + \chi_1^x\chi_0^y|10\rangle + |\varepsilon\rangle, \tag{18}$$

$$|\phi_{n\neq 0}\rangle_{xy} = f_n[\chi_0^x\chi_0^y|00\rangle + (-1)^n\chi_1^x\chi_1^y|11\rangle], \tag{19}$$

where

$$|\varepsilon\rangle = e^{-|\alpha|^2\theta^2/2}(\chi_0^x\chi_0^y|00\rangle + \chi_1^x\chi_1^y|11\rangle) \tag{20}$$

and

$$f_n = \frac{\bar{\alpha}^n}{\sqrt{n!}}e^{-|\alpha|^2\theta^2/2}. \tag{21}$$

The photon number in the upper channel is then measured with single-photon resolution, while the output from the lower channel is left unmeasured. From Eq. (17), the probability of detecting n photons $P(n)$ is given by

$$P(n) = \Lambda\delta_{n,0} + (1-\Lambda)e^{-N\theta^2}\frac{(N\theta^2)^n}{n!}, \tag{22}$$

where $\Lambda = |\chi_0^x\chi_1^y|^2 + |\chi_1^x\chi_0^y|^2$ is the weight of balanced-space states in the initial qubits' state. The probability of detecting zero photons is thus

$$P(0) = \Lambda(1-\varepsilon) + \varepsilon, \tag{23}$$

where $\varepsilon = e^{-N\theta^2}$ indicates the probability of a false null result. On detecting the null result, the qubits' state will collapse onto

$$|\Psi_B\rangle = \frac{1}{\sqrt{\Lambda(1-\varepsilon)+\varepsilon}}[\chi_0^x\chi_1^y|01\rangle + \chi_1^x\chi_0^y|10\rangle + \sqrt{\varepsilon}(\chi_0^x\chi_0^y|00\rangle + \chi_1^x\chi_1^y|11\rangle)]. \tag{24}$$

The fidelity upon this null result f_{nul}, which measures the weight of balanced states in $|\Psi_B\rangle$, is thus

$$f_{nul} = \frac{\Lambda}{\Lambda + (1-\Lambda)\varepsilon}, \tag{25}$$

which is nonunity due to the nonzero probability of a false null result. The condition for faithful teleportation is then $\varepsilon \ll 1$, or $N\theta^2 \gg 1$, characteristic of a standard-quantum-limit interferometer.

The remaining time, a photon number $n \neq 0$ is detected, with the qubit state collapsing onto the imbalanced space with unit fidelity,

$$|\Psi_U\rangle = \frac{1}{\sqrt{1-\Lambda}}[\chi_0^x\chi_0^y|00\rangle + (-1)^n\chi_1^x\chi_1^y|11\rangle]. \tag{26}$$

The $(-1)^n$ term comes from the phase difference between number states for the coherent states $|\alpha\rangle$ and $|-\alpha\rangle$, i.e., while measuring the photon number cannot distinguish the states $|00\rangle$ and $|11\rangle$, it can introduce the relative phase between them. If the photon number is definitely nonzero, yet not measured exactly, then tracing over the photon number creates a statistical mixture of $|00\rangle$ and $|11\rangle$. In this case, the protocol would create an entangled state with nonunity success probability Λ, but success would be heralded by the verification of zero photons in the upper output. Most likely, the initial state $\chi_m^\mu = 1/\sqrt{2}$ would be prepared so that $\Lambda = 50\%$. For entanglement on-demand, however, it is necessary to determine the photon number exactly. This difficulty is somewhat mitigated by the fact that the average photon number is $\bar{n}_0 = -\log_2\varepsilon$, i.e., only five photons must be counted for $\varepsilon = 0.01$ and 7 for $\varepsilon = 0.001$.

Leaving the lower output unmeasured means that computing the output state requires tracing over the lower mode. In the proceeding derivation we have taken this trace to be unity. In reality, it is less than unity due to the nonorthogonality of the balanced and imbalanced lower output states, governed by the overlap

$$|{}_1\langle\bar{\alpha}\cos\theta_{ii}|\bar{\alpha}\cos\theta_{ij}\rangle_1|^2 \approx 1-(1-\delta_{ij})\theta^4 N/8 = 1 - O(1/N). \tag{27}$$

Here, $N = |\alpha|^2$ is the mean input photon number and the last equality is because our scheme requires $N\theta^2 \gg 1$. The resulting error is then $\sim 1/N$, which can be neglected for large N. This result validates the small-angle approximation made for the final state as in Eq. (17), where the lower-channel light field is assumed θ-independent and factorized from the remaining system.

The overall fidelity due to state error in this interferometrical entanglement generation is obtained by averaging over the null and not-null results, giving

$$f_{avg} = P(0)f_{nul} + \sum P(n\neq 0)1 = 1-(1-\Lambda)\varepsilon. \tag{28}$$

Since $\Lambda \geq 0$, it is always $f_{avg} \geq 1-\varepsilon$, regardless of the quantum states of the two qubits.

Aside from the technical challenge of single-photon counting, the fundamental quantum-mechanical barrier to successful teleportation lies in finding a balance between phase-shift detection and spontaneous-emission avoidance, as a single spontaneously scattered photon can destroy the coherence of a qubit. The spontaneous emission probability for a single qubit is $\theta N\Gamma/\Delta$, which becomes negligible when $\theta N\Gamma/\Delta \ll 1$. This condition must be satisfied without violating the shot-noise-sensitivity condition $N\theta^2 \gg 1$. From Eq. (4) it follows that compatibility requires $16(W/\lambda)^2 \ll 1$, which clearly violates the standard optical diffraction limit. That such a scheme can therefore not work is in agreement with common understanding [15].

B. Coherent state input with cavity feedback

To overcome the effects of spontaneous emission, we can place the two qubits in separate high-finesse optical cavities, with mechanical Q switching employed to restrict the photon to M passes through each qubit. This will increase the phase shift θ and the spontaneous emission probability P_{sp} by a factor of M. This relaxes the compatibility condition to $8(W/\lambda)^2 \ll M$, which can be satisfied without subwavelength focusing.

The failure probabilities due to interferometry sensitivity and spontaneous emission are then $\varepsilon = e^{-NM\theta^2}$ and

$$P_{SP} = 2NM\theta\Gamma/\Delta, \tag{29}$$

respectively. Setting $P_{sp} = \varepsilon = 0.01$, corresponding to a fidelity of 0.99, and taking $W/\lambda = 3$ gives

$$M = -144 \log_2 \varepsilon/\varepsilon = 6.6 \times 10^5, \tag{30}$$

which is large but not necessarily outside the range of current experimental techniques. For these parameters, the mean number of photons in the upper output is $\bar{n}_0=4$, and the input photon number is restricted only by the condition $N(\Gamma/\Delta)^2 = 144\varepsilon/M = 4.4\times 10^{-6}$, together with the off-resonant condition $\Delta \gg \Gamma$.

A main difficulty in long-distance quantum communication is photon loss during qubit-to-qubit transmission, where the loss probability increases exponentially with the transport distance. In schemes based on cavity QED [5–8], atomic qubits' states are encoded in the internal (polarization) states of photons, and thus a lost photon will immediately reveal the atomic states and destroy the qubits via decoherence. In contrast, during an interferometrical communication, the qubits' state information is encoded in a form of relative phase shifts of photons propagating in the upper and lower arms. Such a shift is not a measurable quantity until the two channels are recombined at a second beamsplitter. Thus the lost photon cannot reveal the state of the qubit, and one might suspect that the qubit coherence would be preserved. On the other hand, due to the photon-atom interaction, a lost photon will introduce a small relative phase shift to the qubits. The magnitude of the relative phase is θ, but the sign depends on which interferometer arm lost the photon. Tracing over which arm thus results in effective decoherence and thus a reduction in the fidelity of entanglement.

To see this, we first consider one photon lost during propagating between the first and the second qubits. This will alter the final state into

$$|\Psi_f'\rangle = \sqrt{\frac{2}{N}} \hat{U}_{BS} \hat{U}_y \hat{a}_q \hat{U}_x \hat{U}_{BS} |\Psi_i\rangle, \tag{31}$$

with $q=0,1$ corresponding to the loss in upper and lower arms, respectively. The identity

$$\hat{U}_{BS} \hat{U}_y \hat{a}_q \hat{U}_y^\dagger \hat{U}_{BS}^\dagger = e^{i\theta \hat{c}_{yq}^\dagger \hat{c}_{yq}} (\hat{a}_q - i\hat{a}_{1-q})/\sqrt{2} \tag{32}$$

enables us to write

$$|\Psi_f'\rangle = \sqrt{\frac{1}{N}} e^{i\theta \hat{c}_{yq}^\dagger \hat{c}_{yq}} (\hat{a}_q - i\hat{a}_{1-q}) \hat{U} |\Psi_i\rangle \tag{33}$$

$$= (-i)^q e^{i\theta \hat{c}_{yq}^\dagger \hat{c}_{yq}} |\Psi_f\rangle, \tag{34}$$

where in the last step we have used the fact that for the present input state (15), $\hat{a}_q|\Psi_i\rangle = \alpha \delta_{q,0}|\Psi_i\rangle$. It is now clear that the net effect of one lost photon is equivalent to introducing a relative phase $\pm\theta$ to the qubit, where $\theta \ll 1$. In the case of random photon losses, such phase disturbances will lead to the unknown drift of the qubit's state and thus a reduction in the overall fidelity of the entanglement generation. To estimate this fidelity reduction, we introduce the lost photon number distribution $f(k)$. Because each photon is lost independently, $f(k)$ will exhibit a Poisson distribution, where for a mean loss number $\bar{k}$, the variance is $\sqrt{\bar{k}}$. For simplicity, we approximate $f(k)$ with a Gaussian,

$$f(k) = \frac{e^{-(k-\bar{k})^2/2\bar{k}}}{\sqrt{2\bar{k}\pi}}. \tag{35}$$

The system's density ρ^{loss} after the loss is then a mixture of

$$\rho^{loss} = \sum_{k,k'} (-i)^{k'} f(k) f(k') (\hat{P}_0)^k (\hat{P}_1)^{k'} |\Psi_f\rangle\langle\Psi_f| (\hat{P}_1^\dagger)^{k'} (\hat{P}_0^\dagger)^k, \tag{36}$$

where we have introduced the y-qubit projector

$$\hat{P}_q = e^{i\theta \hat{c}_{yq}^\dagger \hat{c}_{yq}} = e^{i\theta} |q\rangle_y\langle q| + |1-q\rangle_y\langle 1-q|. \tag{37}$$

Defining the reduced fidelity due to the photon loss,

$$f_{loss} = \mathrm{tr}\{\rho \rho^{loss}\}, \tag{38}$$

it is found

$$\bar{k} = \frac{N \log_2(2f_{loss} - 1)}{\log_2 \varepsilon}. \tag{39}$$

Taking $f_{loss} = 1-\varepsilon = 0.99$ gives $\bar{k} = 0.004N$, meaning about one photon can be lost in every 250 photons.

In conclusion, in this section we showed that the MZ-interferometrical generation of entanglement using coherent state is quantum-mechanically allowed only with the aid of optical resonators. We found that a fidelity of 0.99 can be achieved using ring cavities which cycle photons for 6.6×10^5 times, with about four photons needing to be measured accurately at one output. Furthermore, we found that unlike most cavity-QED schemes, the present approach can be tolerant of a small photon loss rate.

C. Twin-Fock state input

To achieve a higher fidelity, and/or to eliminate the need for a high-finesse resonator, we now consider using sub-shot-noise interferometers to overcome the spontaneous emission to phase sensitivity. In this section, we investigate the fundamental limits when a twin-Fock (TF) photon input state is used to increase the phase sensitivity of the MZ interferometer. The TF input setup differs in that the photon number difference between the outputs must be measured. In this case, a result of zero number difference constitutes a null result.

The input state is now $|N,N\rangle$, with the dual-Fock basis defined as

$$|k,l\rangle = (\hat{a}_0^\dagger)^k (\hat{a}_1^\dagger)^l |0\rangle / \sqrt{k!\, l!}. \tag{40}$$

The TF input state is then $|N\rangle_0 |N\rangle_1$ with 0, 1 corresponding to upper and lower inputs as before. Following Eq. (16), the output state is now

$$|\Psi_f\rangle = \sum_{ij} \chi_i^x \chi_j^y |ij\rangle \otimes \sum_{m=-N}^{N} \xi_m(\theta_{ij}) |N+m, N-m\rangle, \tag{41}$$

where

$$\xi_m(\theta_{ij}) = \sum_{l=\max\{0,-m\}}^{\min\{N,N-m\}} (-1)^{m+l} \binom{m+l}{N} \binom{l}{N} \times \frac{\sqrt{(N+m)!\,(N-m)!}}{N!} (\sin\theta_{ij})^{m+2l} (\cos\theta_{ij})^{2N-m-2l}.$$

The desired two-qubit entangled state is then created by measuring the photon number difference between the upper and lower outputs. It is seen from Eq. (41) that the probability of detecting a difference of $2m$ is given by

$$P(2m) = \Lambda\delta_{n,0} + (1-\Lambda)\xi_m^2(\theta), \tag{42}$$

where again $\Lambda = |\xi_0^x\chi_1^y|^2 + |\chi_1^x\chi_0^y|^2$. The probability to detect zero photon number difference (or a null result) is thus

$$P(0) = \Lambda(1-\eta) + \eta, \tag{43}$$

where $\eta = \xi_0^2(\theta)$ is the probability of a false null result. On detecting the null result, the qubit state will collapse onto

$$|\Psi_B\rangle = \frac{1}{\sqrt{\Lambda(1-\eta)+\eta}} [\chi_0^x\chi_1^y|01\rangle + \chi_1^x\chi_0^y|10\rangle + \sqrt{\eta}(\chi_0^x\chi_0^y|00\rangle + \chi_1^x\chi_1^y|11\rangle)], \tag{44}$$

with the corresponding fidelity

$$f_{nul} = \frac{\Lambda}{\Lambda + (1-\Lambda)\eta}. \tag{45}$$

The remaining time, a photon number difference $m \neq 0$ is detected, with the qubits collapsed to

$$|\Psi_U\rangle = \chi_0^x\chi_0^y|00\rangle + (-1)^m\chi_1^x\chi_1^y|11\rangle. \tag{46}$$

Here, similar to the coherent state, the exact photon number difference must be measured in order to successfully disentangle the qubits. The overall fidelity in this entanglement generation is then

$$f_{avg} = 1 - (1-\Lambda)\varepsilon \geq 1 - \varepsilon. \tag{47}$$

The TF input thus yields results similar to the coherent-state input, but with the intrinsic error due to interferometer sensitivity given by η instead of ε. A comparison plot of η and ε is shown in Fig. 2, where it is seen that η decreases with N much faster than ε. In fact, for $N\theta < 1$, $\eta \approx e^{-N^2\theta^2}$, which is characteristic of a Heisenberg-limited phase sensitivity. This means that significantly fewer photons are required to obtain equal fidelity, with a corresponding reduction in spontaneous emission. In Fig. 2, we see that the false-null probability η is exactly zero for a periodic set of values of $N\theta$. The first such zero occurs at $N\theta = 1.196 \equiv x_1$. Thus if one can precisely control $N\theta$, *it is possible to achieve teleportation without intrinsic error due to false-null results*. In this case, the success of teleportation is governed only by spontaneous emission probability $P_{sp} = 2N\theta\Gamma/\Delta = 2x_1\Gamma/\Delta$. The condition $N\theta = x_1$, together with Eq. (4), means that $\Gamma/\Delta = (8x_1/N)(W/\lambda)^2$, so that

$$P_{sp} = (16x_1^2/N)(W/\lambda)^2. \tag{48}$$

For the case of a tightly focused beam, we can take $W/\lambda \approx 3$; this gives $P_{sp} = 206/N$. The theoretical limit to fidelity

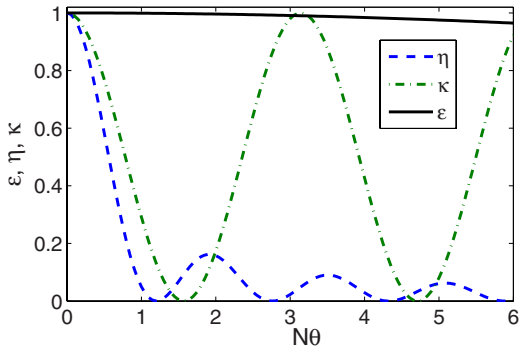

FIG. 2. (Color online) An example of intrinsic error due to interferometer sensitivity. Errors for MZ interferometer with coherent ε (solid), FT input η (dashed), and NOON-state interferometer κ (dashed-dotted) are plotted as functions of $N\theta$ (with $N=10^3$), respectively. Note that while ε is dependent on $N\theta^2$, both η and κ are dependent on $N\theta$.

therefore scales as $\sim 1-200/N$ thus a fidelity of $f=0.99$ would require $N=2\times10^4$ (or a total of 4×10^4 photons), while a fidelity of $f=0.999$ could be achieved with $N=2\times10^5$. An extremely high fidelity of $f=0.999\,999$ would therefore require $N=2\times10^8$. The addition of a Q-switched cavity with M cycles replaces N with the effective photon number MN resulting in the spontaneous emission probability $P_{sp}=206/(NM)$, which for $M=2\times10^4$, would reduce the photon numbers to $N=1$ for $f=0.99$, $N=10$ for $f=0.999$, and $N=10^4$ for $f=0.999\,999$.

The exact elimination of false-null-induced reduction in fidelity requires the precise control of single-particle phase shift θ, as well as the particle number N. Imprecise controls of either will lead to $\eta \neq 0$, and thus a reduction in overall fidelity. To estimate this effect, we let $N\theta = x_1 + \delta$, with δ resulted from the displacement of θ and/or N. Expanding $\eta(x_1+\delta)$ near $\eta(x_1)=0$ gives

$$\eta(x_1+\delta) \approx 1.3\delta^2. \tag{49}$$

For a fidelity of $f=1-200/N$ (with $\eta=200/N$), it requires $\delta < 12.4/\sqrt{N}$. This then requires $\theta_1 - 9.5\theta_1^{1.5} < \theta < \theta_1 + 9.5\theta_1^{1.5}$, where $\theta_1 = x_1/N$ is the desired per-atom phase shift. This allows a relatively flexible control of θ.

Last, we note that for the TF input and the present parameter choice of $N\theta = x_1$, a single photon loss will immediately reduce the fidelity, with a worst-case result of $f=0.73$ and thus disrupt the on-demand entanglement generation scheme. This is because a lost photon will lead to a rapid degradation of the interferometer sensitivity. To see this, for the TF input state, one photon lost from the qth path during qubit-to-qubit propagation will result in the final state,

$$|\Psi_f'\rangle = \sqrt{\frac{1}{N}}\hat{U}_{BS}\hat{U}_y\hat{a}_q\hat{U}_x\hat{U}_{BS}|\Psi_i\rangle. \tag{50}$$

Using the identity (32), we find

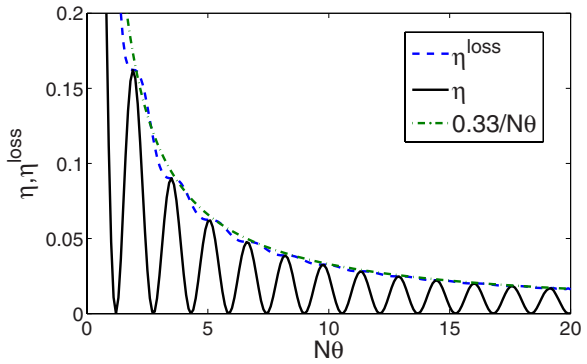

FIG. 3. (Color online) Comparison of η^{loss} and η. Note that both depend only on the product $N\theta$.

$$|\Psi_f'\rangle = \sqrt{\frac{1}{2N}}[e^{i\theta\hat{c}_{yq}^{\dagger}\hat{c}_{yq}}(\hat{a}_q - i\hat{a}_{1-q})]\hat{U}|\Psi_i\rangle, \tag{51}$$

$$= \sqrt{\frac{1}{2N}}\sum_{ij}\chi_i^x\chi_j^y\hat{P}_q|ij\rangle \otimes \sum_{m=-N}^{N}\xi_m(\theta_{ij})$$
$$\times[(-i)^q\sqrt{N+m}|N+m-1,N-m\rangle$$
$$+(-i)^{1-q}\sqrt{N-m}|N+m,N-m-1\rangle],$$

with the projector $\hat{P}_q$ defined in Eq. (37). A lost photon will therefore result in odd number differences of photons measured in the two output ports. Since without photon loss, a TF state will always result in even number differences, it is in this way possible to determine the loss of a single photon (without knowing which path it is lost from). Seemingly, this makes it possible to detect the phase imbalance if we accordingly redefine a null result as the measured photon number difference being 1. The false-null rate, as given by

$$\eta^{loss} = |\xi_0(\theta) + i\xi_1(\theta)\sqrt{1+1/N}|^2, \tag{52}$$

is, however, no long a small quantity. A comparison of η^{loss} and η is plotted in Fig. 3, where it is shown that η^{loss} behaves as the envelope of η without the zero-value points. In particular, with the present choice of $N\theta=x_1$, it is found $\eta^{loss}\approx 0.27$, in contrast to the corresponding rate $\eta=0$ without the loss. Depending on the qubits' states, a photon loss will thus immediately degrade the fidelity to $f\geq 0.73$.

On the other hand, η^{loss} is yet much smaller than the corresponding false-null rate ε for the coherent state. Hence if we presume one photon will be lost and set the value of $N\theta$ accordingly, we may still generate entanglement without the cavity enhancement. In fact, as shown in Fig. 3, a least-square fit finds

$$\eta^{loss} = \frac{0.33}{N\theta}. \tag{53}$$

Letting $\eta^{loss}=P_{sp}$ and using Eq. (4) gives

$$P_{sp} = \frac{2.6}{N^{1/3}}, \tag{54}$$

for $W/\lambda=3$. The limit to fidelity thus scales as $1-2.6/N^{1/3}$, and a fidelity of $f=0.99$ will require $N=1.8\times 10^7$, compared to $N=2\times 10^4$ without photon loss. Entanglement can in this sense still be generated without the need of cavities, while the single-photon loss can be compensated by using more photons. Last, we note that $f\sim 1-2.6/N^{1/3}$ is also the lower limit on the fidelity achievable when the phase shift cannot be tuned such that $\eta(N\theta)=0$. This is simply because η^{loss} is the envelope of η, and for any N and θ, $\eta\leq\eta^{loss}$.

In conclusion, in this section we have shown that for a MZ interferometer with the TF input, atom-atom entanglement can be generated with much higher fidelity, and the need for high-finesse optical resonators can in principle be eliminated. Particularly, we found that a fidelity of 0.99 is quantum-mechanically allowed with 20 000 photons, or more intriguingly with only two photons, provided ring cavities which cycle photons 2×10^4 times are additionally incorporated. The two-photon TF state could be generated with a pair of single-photon-on-demand sources (one for each input) and a precise photon detector to measure the two-photon output state, technologies that are rapidly advancing at present. Finally, we have shown that the present scheme is relatively insensitive to deviations in the per-atom phase shift, yet is highly sensitive to loss of a single photon. This is somewhat mitigated by the fact that for the two-photon state, the loss of a photon could be readily detected, so that success is heralded by the detection of both photons.

IV. NOON-STATE INTERFEROMETER

In above sections, we have discussed generating entanglement between atomic qubits using an optical MZ interferometer with coherent and TF input states. While both are shown to be able to achieve a close-to-unit fidelity in the presence of intrinsic quantum errors, they require precise measurement of output light field at the single-photon level. In this section, we show that this requirement can be overcome by using a non-MZ interferometer based on NOON states and nonlinear beamsplitters [31].

A NOON state is a macroscopic quantum superposition (Schrödinger cat) state that corresponds to an equally weighted superposition of all-upper-channel and all-lower-channel states [21,32–35],

$$|\text{NOON}\rangle = \frac{1}{\sqrt{2}}(|N,0\rangle + e^{i\phi}|0,N\rangle), \tag{55}$$

where ϕ is the relative phase which we take for zero for simplicity. The nonlinear beamsplitter can either be a four-wave mixer [22,36] or a quantum circuit constructed from controlled NOT (CNOT) gates [1]. Without further explaining its operational mechanism or examining the practical feasibility, for the present we simply treat the action of such beamsplitters with a projecting operator $\hat{U}_{NBS}$ of the general form

$$\hat{U}_{NBS} = \frac{1}{\sqrt{2}} \sum_{s} (e^{i\phi}|s,0\rangle + |s,0\rangle)\langle 0,s| + e^{i\varphi}(e^{i\phi}|s,0\rangle - |0,s\rangle)\langle 0,s|,$$

where for simplicity we let the relative phases $\phi=\varphi=0$. Note that for the four-wave mixer, this projector is valid only for even-number s. Using this nonlinear beamsplitter, a NOON state can be generated from a single Fock state $|N,0\rangle$, i.e., by injecting N photons in its upper input channel.

The setup of the NOON-state interferometer differs from a MZ interferometer in that now the first beamsplitter is dropped (or more precisely, it is formally replaced by the assumption of a NOON input state) while the second one is replaced by the nonlinear beamsplitter, as shown in Fig. 1(b). For measurement, a photon detector is placed in the lower (or equivalently, the upper) output port to detect the presence of outcoming photons, without counting them. Because the output light field consists of $|N,0\rangle$ and $|0,N\rangle$ states, corresponding to all photons coming out from the upper or lower port, a photon detector with a resolution of $<N/2$ would be sufficient to distinguish them. This exhibits an essential improvement from the previous MZ interferometry schemes, where the detector resolution must be less than 1. A null result, meaning no photon is detected at the lower channel, will collapse the qubits onto

$$\chi_0^x\chi_1^y|01\rangle + \chi_1^x\chi_0^y|10\rangle + |\kappa\rangle, \tag{56}$$

with $|\kappa\rangle$ the intrinsic state error due to a false-null result. In contrast, if a photon is detected, the qubits will collapse into the imbalanced subspace,

$$\chi_0^x\chi_0^y|00\rangle + \chi_1^x\chi_1^y|11\rangle. \tag{57}$$

Here, we emphasize that this state is independent on the exact number difference n between the upper and lower outputs. This is essentially different from the corresponding ones in Eq. (26) with the coherent state and in Eq. (46) with the TF state, both of which are dependent on n.

To derive these results, we follow the previous approach and find the final state of system as

$$|\Psi_f\rangle = \hat{U}_{NBS}\hat{U}_y\hat{U}_x\left[\frac{1}{\sqrt{2}}(|N,0\rangle + |0,N\rangle) \otimes |\psi_x\rangle \otimes |\psi_y\rangle\right] = \sum_{i,j=0,1} \chi_i^x\chi_j^y|ij\rangle \otimes [\cos N\theta_{ij}|N,0\rangle - i \sin N\theta_{ij}]|0,N\rangle,$$

where we have dropped an irrelevant global-phase term in the last step. The probability of a null result is thus

$$P_{null} = \Lambda(1-\kappa) + \kappa, \tag{58}$$

with $\kappa=\cos^2 N\theta$ the intrinsic error rate. On detecting this null result, the qubits will collapse onto

$$|\Psi_B\rangle = \frac{1}{\sqrt{\Lambda(1-\kappa)+\kappa}}[\chi_0^x\chi_1^y|01\rangle + \chi_1^x\chi_0^y|10\rangle + \sqrt{\kappa}(\chi_0^x\chi_0^y|00\rangle + \chi_1^x\chi_1^y|11\rangle)], \tag{59}$$

where $\kappa=\cos^2 N\theta$ is the false null rate. The corresponding fidelity is then

$$f_{nul} = \frac{\Lambda}{\Lambda + (1-\Lambda)\kappa}. \tag{60}$$

The remaining time, a non-null result is detected, projecting the qubits onto the imbalanced subspace,

$$|\Psi_U\rangle = \frac{1}{\sqrt{1-\Lambda}}(\chi_0^x\chi_0^y|00\rangle + \chi_1^x\chi_1^y|11\rangle). \tag{61}$$

The overall fidelity averaging over the null and non-null results is given by

$$f_{avg} = 1 - (1-\Lambda)\kappa. \tag{62}$$

The fidelity in this entanglement generation is thus similar to the MZ interferometry cases but with the intrinsic error rate given by κ. A comparison of $\varepsilon, \eta, \kappa$ is shown in Fig. 2, where it is shown that for $N\theta<1$, κ is close to η, exhibiting a Heisenberg-limited phase sensitivity. Furthermore, κ is exactly zero at $N\theta=\pi/2$, compared to 1.196 for η. This means the NOON-state interferometer can achieve similar performances with the TF state. The fidelity after taking into account the possibility of spontaneous emission therefore scales as $f\approx 1-350/N$. A fidelity of $f=0.99$ and $f=0.999$ will then require $N=3.5\times 10^4$ and $N=3.5\times 10^5$ photons, respectively. Since there is no requirement on exactly counting output photons, N can in principle be made large, allowing an arbitrary close-to-unit fidelity, at least quantum mechanically. Finally, similar to the TF state, in order to suppress a false-null rate, for a fidelity of $\approx 1-350/N$, θ must be tuned within an interval of $(\theta_1-8.1\theta_1^{1.5}, \theta_1+8.1\theta_1^{1.5})$ with $\theta_1=\pi/2N$.

The present entanglement generation using NOON states will be completely disrupted by a single-photon loss. This is due to the fact that a randomly lost photon will immediately collapse the NOON state to a statistical mixture of all-upper-channel and all-lower-channel states, whose reduced density is given by

$$\rho^{loss} = \frac{1}{2}(|N-1,0\rangle\langle N-1,0| + |N-1,0\rangle\langle N-1,0|). \tag{63}$$

This mixture state is apparently incapable of detecting phase imbalances. This problem, however, might be overcome by using a class of less-extreme catlike states [37,38]. Such a states corresponds to a symmetric superposition of two well-separated wave packets in number-difference space. In the case of small photon losses, instead of being completely destroyed, they will decay into a mixture of smaller-sized catlike states, which are still suitable for the purpose of detecting phase imbalance. Hence aside from a reduction in fidelity due to phase randomization, faithful entanglement might be generated despite photon loss. A further study of generating entanglement using less-extreme catlike states will be presented in future work.

Finally, we note that the present NOON-state interferometer relies on a highly nonclassical light source with a definite photon number. This requirement is, however, not necessary. For example, our scheme can be directly extended to use more "classical" cat input states that correspond to the superposition of coherent states,

$$|\alpha\rangle_0 \otimes |0\rangle_1 + |0\rangle_0 \otimes |\alpha\rangle_1. \tag{64}$$

Such a state can be rewritten as

$$\sum_m f(m)(|m,0\rangle + |0,m\rangle), \tag{65}$$

where $f(m)$ is the coefficient of the coherent state and can be approximated by

$$f(m) = \frac{1}{\sqrt{\mathcal{N}}} e^{-(m-N)^2/4N}, \tag{66}$$

where $\mathcal{N}$ is the normalization factor. A probabilistic scheme to generate this state but containing only even m's has been proposed, with a success probability of 0.5, where a single coherent light and a four-wave mixer are employed [22]. With this input, the final state of the system becomes

$$|\Psi_f\rangle = \sum_{i,j=0,1} \chi_i^x \chi_j^y |ij\rangle \otimes \sum_m f(m)[\cos m\theta_{ij}|m,0\rangle - i \sin m\theta_{ij}] \times |0,m\rangle. \tag{67}$$

By choosing $N\theta = \pi/2$, similar to the single NOON state, upon detecting photons from the lower port, the qubit will collapse to imbalanced subspace (61). Otherwise, if no photon is detected from the lower port, the qubits will collapse to the state (59) but with the false null rate given by

$$\kappa' = \frac{1}{2\mathcal{N}} \sum_m e^{-(m-N)^2/2N}(1 + \cos m\theta) = \frac{1}{2}(1 - e^{-\theta^2 N/2}). \tag{68}$$

Since $N\theta = \pi/2$, we have $\kappa' \approx \pi^2/16N$, which is negligible compared to the fidelity reduction ($\approx 350/N$) due to the probability of spontaneous emission.

To conclude, in this section we have shown that a NOON-state interferometer can achieve similar performance with the TF state, yet without the requirement for precisely measuring the output light field. While this scheme is not tolerant of a single photon loss, this problem might be overcome by using a class of less extreme cat states. Also, besides using a single NOON input state with definite photon number, we have shown that the present scheme can also use a class of states with indefinite photon number that correspond to the superposition of NOON states.

V. EXAMPLES OF APPLICATIONS

The present interferometrical method of generating entanglement can serve as a basic protocol in the quantum information processing, based on which quantum computation and communication can be realized with the aid of local qubit operations. As an example, here we first show how it can be used to teleport an arbitrary quantum state from one qubit to another. We assume the x qubit is the source qubit carrying an unknown teleporting quantum state, and the y qubit is the target qubit to which the state is transported. The x qubit is initially in the state

$$|\psi_x\rangle = \chi_0^x |0\rangle_x + \chi_1^x |1\rangle_x, \tag{69}$$

while the y qubit is initially prepared as

$$|\psi_y\rangle = \frac{1}{\sqrt{2}}(|0\rangle_y + |1\rangle_y). \tag{70}$$

We first collapse the two qubits into entangled qubit pair interferometrically using our method. Once the qubit pair is generated, completing the teleportation requires that the qubits be disentangled. This can be accomplished in the following manner. Conditional upon a null result, a π pulse is applied to the source qubit, flipping $|0\rangle_x \leftrightarrow |1\rangle_x$. When using a MZ interferometer with the coherent or TF state, in the case of an odd measured n, an additional relative π phase must be applied to the state $|1\rangle_x$ (or $|1\rangle_y$). After these steps, the qubits' state becomes

$$\chi_0^x |00\rangle + \chi_1^x |11\rangle. \tag{71}$$

A $\pi/2$ pulse is then applied to the source (or the target) qubit, transforming the state into

$$[\chi_0^x|00\rangle - i\chi_0^x|10\rangle - i\chi_1^x|01\rangle + \chi_1^x|11\rangle]/\sqrt{2}. \tag{72}$$

This is followed by a state measurement of the x qubit. If it is measured $|0\rangle_x$, the y qubit will collapse to

$$\chi_0^x |0\rangle_y - i\chi_1^x |1\rangle_y, \tag{73}$$

after which a $\pi/2$ phase is imprinted onto $|1\rangle_y$. Otherwise, it is measured in $|1\rangle_x$, and a $\pi/2$ phase is imprinted onto $|0\rangle_y$. After these conditional operations, the y qubit will end up in the desired state,

$$\chi_0^x |0\rangle_y + \chi_1^x |1\rangle_y, \tag{74}$$

which accomplishes the teleportation.

Besides the state teleportation between two qubits, our scheme can be easily generalized to generate many-qubit entanglement [39] as well as realize entanglement swapping [40,41]. For example, the three-particle Greenberger-Horne-Zeilinger (GHZ) state,

$$(|000\rangle_{xyz} + |111\rangle_{xyz})/\sqrt{2}, \tag{75}$$

can be created by first preparing each qubit in the state

$$|\psi_\mu\rangle = \frac{1}{\sqrt{2}}(|0\rangle_i + |1\rangle_i), \tag{76}$$

with $i = x, y, z$. Then the two-qubit protocol is used to collapse x and y into the state

$$(|00\rangle_{xy} + |11\rangle_{xy})/\sqrt{2} \otimes (|0\rangle_z + |1\rangle_z)/\sqrt{2}. \tag{77}$$

If the same two-qubit procedure is applied to B and C, the GHZ state is obtained. This simple scheme can be extended in a straightforward manner to producing an N-particle Shrödinger cat state.

To realize entanglement swapping, we take an initially entangled qubit pair,

$$\frac{1}{\sqrt{|c_{00}|^2 + |c_{11}|^2}}(c_{00}|00\rangle_{xy} + c_{11}|11\rangle_{xy}), \tag{78}$$

and an uncorrelated third qubit

$$|\psi_z\rangle = \frac{1}{\sqrt{2}}(|0\rangle_z + |1\rangle_z) \tag{79}$$

and apply our protocol to qubits y and z to create a GHZ-like state. Then, by disentangling y in the same manner as described for the source qubit in teleportation, we arrive at the desired swapped state,

$$\frac{1}{\sqrt{|c_{00}|^2 + |c_{11}|^2}}(c_{00}|00\rangle_{xz} + c_{11}|11\rangle_{xz}). \tag{80}$$

VI. CONCLUSION

In conclusion, we have used the formalism of the optical interferometer to treat the problem of creating entanglement among single-atom qubits via a common photonic channel. We have compared the results from a MZ interferometer with a coherent input state and high-finesse cavity enhancement, a MZ interferometer with TF input, and those from a non-MZ interferometer based on the NOON state and nonlinear beamsplitter. Our results suggest that high-fidelity entanglement can in principle be generated via any of the interferometrical approaches. Experimental feasible schemes under current techniques are found by combining a Heisenberg-limited interferometer with photon resonators. In particular, we find that a two-photon input state has a fundamental upper limit to fidelity of 0.99, and provides the advantage that failure due to photon losses could be readily detected. Our interferometrical approaches of generating entanglement is operated on demand and is scalable, and thus can serve as a universal protocol in quantum information processing, based on which quantum computation and communication can be realized with the aid of single-qubit operations.

ACKNOWLEDGMENTS

This work was supported in part by National Science Foundation Grant No. PHY0653373.

[1] M. A. Nielsen and I. L. Chuang, *Quantum Computation and Quantum Information* (Cambridge University Press, Cambridge, UK, 2000).
[2] C. H. Bennett, G. Brassard, C. Crepeau, R. Jozsa, A. Peres, and W. K. Wootters, Phys. Rev. Lett. **70**, 1895 (1993).
[3] D. Bouwmeester, J.-W. Pan, K. Mattle, M. Eibl, H. Weinfurter, and A. Zeilinger, Nature (London) **390**, 575 (1997).
[4] I. Marcikic, H. de Riedmatten, W. Tittel, H. Zbinden, and N. Gisen, Nature (London) **421**, 509 (2003).
[5] S. Bose, P. L. Knight, M. B. Plenio, and V. Vedral, Phys. Rev. Lett. **83**, 5158 (1999).
[6] S.-B. Zheng and G.-C. Guo, Phys. Rev. A **73**, 032329 (2006).
[7] L.-M. Duan and H. J. Kimble, Phys. Rev. Lett. **90**, 253601 (2003).
[8] T. Di, A. Muthukrishnan, M. O. Scully, and M. S. Zubairy, Phys. Rev. A **71**, 062308 (2005).
[9] M. Riebe, H. Häffner, C. F. Roos, W. Hänsel, J. Benhelm, G. P. T. Lancaster, T. W. Körber, C. Becher, F. Schmidt-Kaler, D. F. V. James, and R. Blatt, Nature (London) **429**, 734 (2004).
[10] M. D. Barrett, J. Chiaverini, T. Schaetz, J. Britton, W. M. Itano, J. D. Jost, E. Knill, C. Langer, D. Liebfried, R. Ozeri, and D. J. Wineland, Nature (London) **429**, 737 (2004).
[11] L.-M. Duan, J. I. Cirac, P. Zoller, and E. S. Polzik, Phys. Rev. Lett. **85**, 5643 (2000).
[12] B. Julsgaard, A. Kozhekin, and E. S. Polzik, Nature (London) **413**, 400 (2001).
[13] D. N. Matsukevich and A. Kuzmich, Science **306**, 663 (2004).
[14] P. van Loock, T. D. Ladd, K. Sanaka, F. Yamaguchi, Kae Nemoto, W. J. Munro, and Y. Yamamoto, Phys. Rev. Lett. **96**, 240501 (2006).
[15] S. J. van Enk and H. J. Kimble, Phys. Rev. A **63**, 023809 (2001).
[16] B. Yurke, S. L. McCall, and J. R. Klauder, Phys. Rev. A **33**, 4033 (1986).
[17] M. J. Holland and K. Burnett, Phys. Rev. Lett. **71**, 1355 (1993).
[18] L. Pezzé and A. Smerzi, Phys. Rev. A **73** 011801(R) (2006).
[19] A. Heidmann, R. J. Horowicz, S. Reynaud, E. Giacobino, C. Fabre, and G. Camy, Phys. Rev. Lett. **59**, 2555 (1987).
[20] B. Lantz, P. Fritschel, H. Rong, E. Daw, and G. González, J. Opt. Soc. Am. A **19**, 91 (2002).
[21] J. J. Bollinger, Wayne M. Itano, D. J. Wineland, and D. J. Heinzen, Phys. Rev. A **54**, R4649 (1996).
[22] C. C. Gerry, Phys. Rev. A **61**, 043811 (2000).
[23] W. J. Munro, K. Nemoto, G. J. Milburn, and S. L. Braunstein, Phys. Rev. A **66**, 023819 (2002).
[24] S. F. Huelga, C. Macchiavello, T. Pellizzari, A. K. Ekert, M. B. Plenio, and J. I. Cirac, Phys. Rev. Lett. **79**, 3865 (1997).
[25] C J. Hood, H. J. Kimble, and J. Ye, Phys. Rev. A **64**, 033804(R) (2001).
[26] J. M. Raimond, M. Brune, and S. Haroche, Rev. Mod. Phys. **73**, 565 (2001).
[27] A. Kuhn, M. Hennrich, and G. Rempe, Phys. Rev. Lett. **89**, 067901 (2002).
[28] W. T. M. Irvine, K. Hennessy, and D. Bouwmeester, Phys. Rev. Lett. **96**, 057405 (2006).
[29] Z. Hradil and J. Řeháček, Phys. Lett. A **334**, 267 (2005).
[30] L. Pezzé and A. Smerzi, Europhys. Lett. **78**, 30004 (2007).
[31] T. Kim, J. Dunningham, and K. Burnett, Phys. Rev. A **72**, 055801 (2005).
[32] X.-B. Zou, J. Kim, and H.-W. Lee, Phys. Rev. A **63**, 065801 (2001).
[33] M. W. Mitchell, J. S. Lundeen, and A. M. Steinberg, Nature (London) **429**, 161 (2004).
[34] C. C. Gerry and R. A. Campos, Phys. Rev. A **64**, 063814 (2001).
[35] H. Lee, P. Kok, N. J. Cerf, and J. P. Dowling, Phys. Rev. A **65**, 030101(R) (2002).
[36] B. Yurke, S. L. McCall, and J. R. Klauder, Phys. Rev. A **33**, 4033 (1986).

[37] A. Micheli, D. Jaksch, J. I. Cirac, and P. Zoller, Phys. Rev. A **67**, 013607 (2003).

[38] Y. P. Huang and M. G. Moore, Phys. Rev. A **73**, 023606 (2006).

[39] D. M. Greenberger, M. Horne, and A. Zeilinger, in *Bell's Theorem, Quantum Theory, and Conceptions of the Universe*, edited by M. Kafatos (Kluwer, Dordrecht, 1989), p. 73–76.

[40] J.-W. Pan, D. Bouwmeester, H. Weinfurter, and A. Zeilinger, Phys. Rev. Lett. **80**, 3891 (1998).

[41] L.-M. Duan, M. D. Lukin, J. I. Cirac, and P. Zoller, Nature (London) **414**, 413 (2001).